

Synthesis of nitrogen-doped, graphene-supported gold nanoparticles via a microwave irradiation method and their electrochemical properties

Kun Zhang¹ · Jimei Zhang¹ · Shibo Qi¹

Received: 18 May 2015 / Accepted: 26 September 2015 / Published online: 24 October 2015
© Springer Science+Business Media Dordrecht 2015

Abstract In this paper, nitrogen-doped graphene (N-G) was first produced by an eco-friendly hydrothermal method using low-cost industrial material $(\text{NH}_4)_2\text{CO}_3$ as the nitrogen source. Nitrogen-doped, graphene-supported gold (Au/N-G) nanoparticles (NPs) were synthesized through the reduction of HAuCl_4 using sodium citrate as the reducing agent by a microwave irradiation process. The N-G and Au/N-G NPs were characterized by scanning electron microscopy, transmission electron microscopy, X-ray diffraction and X-ray photoelectron spectroscopy. The results indicated that gold nanoparticles (AuNPs) were effectively loaded on the surface of N-G. Cyclic voltammetry and electrochemical impedance spectroscopy of the Au/N-G NPs suggested they are an excellent electrode material with good electrochemical properties.

Keywords Nitrogen-doped graphene · Au nanoparticles · Microwave irradiation · Electrochemical

Introduction

Graphene has attracted considerable interest due to its outstanding electrical conductivity, good electrochemical stability and large specific surface area [1, 2]. Many methods have been applied to improve the physicochemical properties of graphene, such as chemical functionalization, graphene hybrids and chemical

✉ Jimei Zhang
zhangjimei6d311@163.com
Kun Zhang
zyzk0510@163.com

¹ State Key Laboratory of Hollow Fiber Membrane Materials and Membrane Process, Tianjin Polytechnic University, Tianjin 300387, People's Republic of China

doping with heteroatoms [3]. Among these methods, chemical doping is considered an effective way to increase the density of charge-carrier and electrical conductivities [4]. Recently, doping graphene with heteroatoms, such as boron [5], nitrogen [6, 7], sulfur [8, 9], has been used to produce functionalized graphene for electrochemical applications.

Nitrogen is considered a potential element for chemical doping because of its similar atom size and five valence electrons that can form valence bonds with carbon atoms [10]. Several nitrogen sources have been used to prepare N-G, including nitrogen plasma [11], ammonia [12, 13], acetonitrile [14], melamine [3, 15] and urea [16, 17]. It is difficult to control the doping structure of N-G with these nitrogen sources and the content of nitrogen is low. Herein, we prepared N-G sheets by a hydrothermal reaction at a relatively low temperature with $(\text{NH}_4)_2\text{CO}_3$ as a nitrogen source [18].

Noble metal NPs such as Au, Ag and Pt have been deposited on N-G to obtain novel nano-composites which showed good electrochemical activity and stability [19–23]. Due to the strong binding force between AuNPs and N-G, AuNPs were uniformly deposited on N-G via a microwave radiation method.

In this work, N-G was synthesized via a hydrothermal method and used as raw material to prepare Au/N-G NPs. The as-prepared hybrid materials were characterized by various technologies, including scanning electron microscopy (SEM), transmission electron microscopy (TEM), X-ray diffraction (XRD) and X-ray photoelectron spectroscopy (XPS). Electrochemical properties were tested by cyclic voltammetry (CV) and electrochemical impedance spectroscopy (EIS) methods.

Experimental section

Reagents

All reagents were of analytical grade and without further purification. Graphite powders were the products of the Qingdao Colloid Graphite Co., Ltd. (China). KMnO_4 , H_2SO_4 and NaNO_3 were obtained from Tianjin Guangfu Science and Technology Co., Ltd. (China). $(\text{NH}_4)_2\text{CO}_3$ powders were purchased from Tianjin Guangfu Fine Chemical Research Institute. H_2O_2 and $\text{K}_3[\text{Fe}(\text{CN})_6]$ were achieved from Tianjin Fengchuan Chemical Reagent Technologies Co., Ltd. (China).

Apparatus

All electrochemical measurements were performed on a VersaSTAT3 electrochemical workstation (Princeton Instruments Co., Ltd., US) with a standard three-electrode system containing a platinum wire auxiliary electrode, an Ag/AgCl reference electrode and the modified glassy carbon electrode as the working electrode. SEM images of samples were performed on a X-50 field-emission scanning electron microscopy (FE-SEM) instrument. The morphology of N-G and Au/N-G NPs were characterized by TEM (Hitachi-7650) with an accelerating voltage of 100 kV. XRD (Rigaku D/max-2500, Cu $\text{K}\alpha$ radiation) was used to

determine the phase purity and crystallization degree. XPS analysis was carried out on a K-alpha spectrometer (Thermo Fisher Scientific Co., Ltd, US). The microwave reactor was purchased from Gongyi City Instrument Co., Ltd. (China). All measurements were carried out at room temperature.

Preparation of graphene oxide (GO) and N-G

Graphene oxide (GO) was prepared via the modified Hummers' method by the oxidation of flake graphite powders [24, 25], and N-G was synthesized using $(\text{NH}_4)_2\text{CO}_3$ as a functional agent [18]. The GO was suspended in 50 mL of water to yield a brown colloidal dispersion with a concentration of 2 mg mL^{-1} , and 10.0 g of $(\text{NH}_4)_2\text{CO}_3$ powders were dissolved in the solution. Stirring 20 min, the obtained solution was sealed in a 100-mL Teflon-lined autoclave and maintained at $130 \text{ }^\circ\text{C}$ for 10 h. After cooling to room temperature, the sample was centrifuged and washed with distilled water several times. Finally, the collected solids were dried in a vacuum desiccator at $60 \text{ }^\circ\text{C}$.

Preparation of Au/N-G NPs

In a typical synthetic process, 20 mg of N-G was ultrasonically dispersed in 40 mL of water and gave a suspension. 100 μL of 1 % HAuCl_4 and 2.0 mL 0.1-mol L^{-1} sodium citrate were added into the suspension. Stirring for 0.5 h, the mixture was transferred into a round-bottomed flask and heated to $80 \text{ }^\circ\text{C}$ under constant stirring. After 30 min of microwave radiation at 800 W, the product was collected by centrifugation, washed with water several times, and dried in a vacuum desiccator at $60 \text{ }^\circ\text{C}$.

GO, N-G and Au/N-G NPs modified glassy carbon electrode

The glassy carbon electrode (GCE) surface was polished with $0.3\text{-}\mu\text{m}$ alumina, and washed successively with ultrapure water, 1:1 anhydrous alcohol and ultrapure water in an ultrasonic bath and dried in an N_2 atmosphere. 5 μL of 0.5-mg mL^{-1} N-G suspension, prepared by dispersing N-G in chitosan (1 % v/v) with 2 h of ultrasonic dispersion, was coated on the electrode surface to obtain N-G/GCE and dried under $50 \text{ }^\circ\text{C}$ for 10 min. The GO and Au/N-G NPs-modified GCE were prepared by the same method.

Results and discussion

SEM analysis of N-G and Au/N-G NPs

The morphology and structure of N-G and Au/N-G NP samples were characterized by SEM. As shown in Fig. 1a, N-G exhibited curved and layer-like shapes with a highly crumpled and three dimensional (3D) architecture, which can provide a

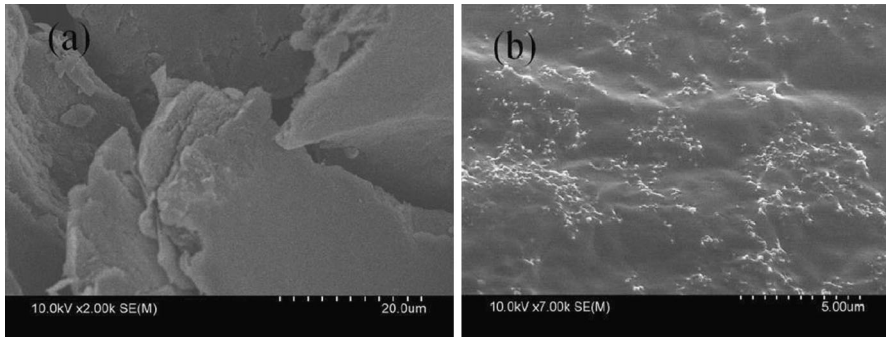


Fig. 1 SEM images of N-G (a) and Au/N-G NPs (b)

skeleton for AuNPs. Comparing to N-G, Au/N-G NPs displayed a distinct crumpled structure and maintained typical sheet-like morphology. It can be observed that the N-G sheets were highly decorated with AuNPs in crumpled sites. The unique structure of Au/N-G NPs maintained a high surface area, which was good for electron transport and electrochemical activity.

TEM analysis of N-G and Au/N-G

Figure 2a revealed that N-G was randomly compacted and stacked together, showing uniform laminar morphology like crumpled silk veil waves. The morphology was attributed to the defects formed upon exfoliation or the presence of doped nitrogen [26]. The wrinkled structure of N-G provided a large surface area for AuNPs and played an important role in preventing N-G sheets from aggregating. In Fig. 2b, AuNPs were well-dispersed on N-G substrates. The decorated AuNPs were spherical and the diameter ranged from 8 to 25 nm. The average size of AuNPs on N-G was ca. 15.22 nm as determined via mathematical statistics. The corresponding particle size distribution of AuNPs was shown in Fig. 2c; Au nanoparticles were uniformly distributed on N-G sheets, which was good for catalytic activity and sensor sensitivity [27].

XRD analysis of GO, N-G and Au/N-G NPs

The XRD peak positions have been used to investigate phase identification and calculate the interlayer spacing distance. In Fig. 3a, GO had a sharp peak at 12.1° , corresponding to a layered structure with a basal spacing of 0.736 nm. As shown in Fig. 3b, a broad diffraction peak was found to shift to $2\theta = 25^\circ$ ($d = 0.365$ nm), which is attributed to the (002) plane of graphite. The disappearance of the sharp peak indicated that oxygen-containing functional groups were sufficiently reduced. After Au NP loading on the N-G, the appearance of the strong diffraction peaks at 2θ values of 38.2° , 44.6° , 64.7° and 77.5° (Fig. 3c) belonging to the (111), (200), (220) and (311) crystal planes of the face-centered cubic structure of Au,

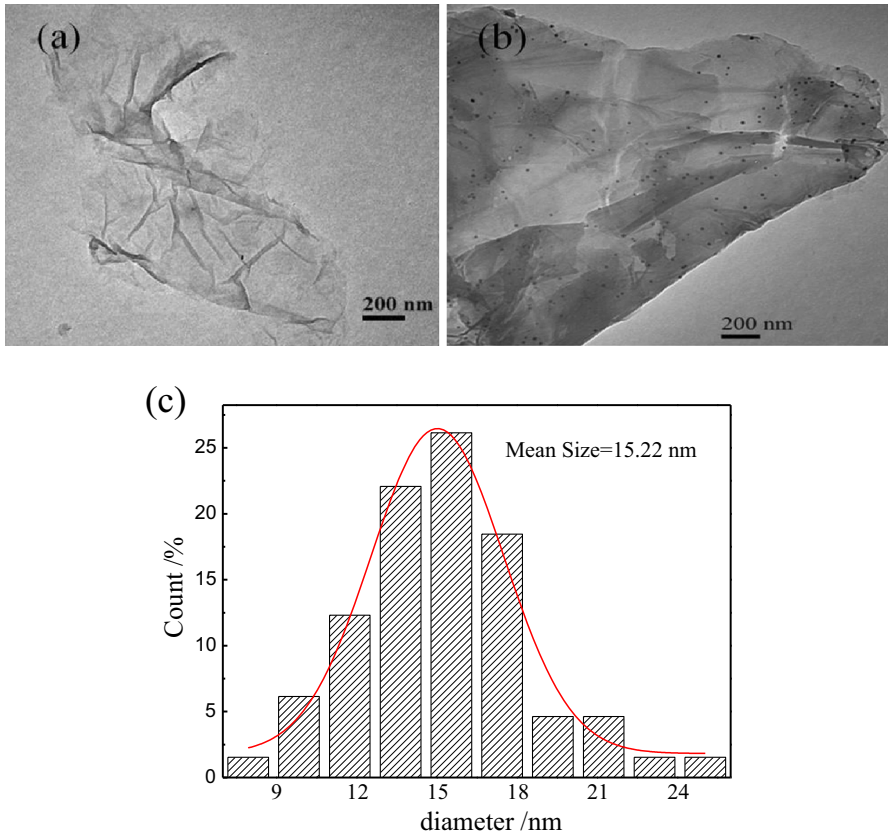


Fig. 2 TEM images of N-G (a), Au/N-G NPs (b) and corresponding particle size distribution (c)

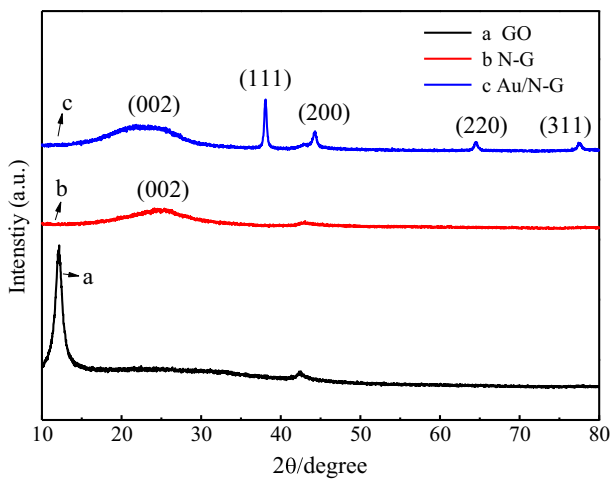


Fig. 3 XRD patterns of GO (a), N-G (b) and Au/N-G NPs (c)

respectively. The diffraction line of the support material N-G almost had no change, which indicated that the Au loading had no effect on the structure of the support material [19].

XPS analysis of N-G and Au/N-G NPs

The surface morphology and chemical element states of N-G and Au/N-G NPs have been further tested by XPS. In Fig. 4a, the representative full spectrum of N-G exhibited three peaks centered at 285.1, 399.1 and 532.1 eV, corresponding to C 1s, N 1s and O 1s, respectively. The appearance of N 1s peak revealed that nitrogen was successfully doped into the graphene lattice and nitrogen content was detected to be about 7.9%. According the literature [28], the N 1s peak (Fig. 4b) could be resolved into three constituents: pyridinic N (~ 398.2 eV), pyrrolic N (~ 399.5 eV), graphitic N (~ 401.3 eV). For the Au/N-G NP sample (Fig. 4c), the main feature peaks were ascribed to C 1s, N 1s, O 1s and Au 4f core levels. Moreover, the two intense peaks between N 1s and C 1s could be attributed to Au 4d. In the high-resolution XPS spectrum of Au (Fig. 4d), two peaks of the Au 4f core level at 87.16 and 83.42 eV were attributed to Au 4f_{5/2} and Au 4f_{7/2}, respectively.

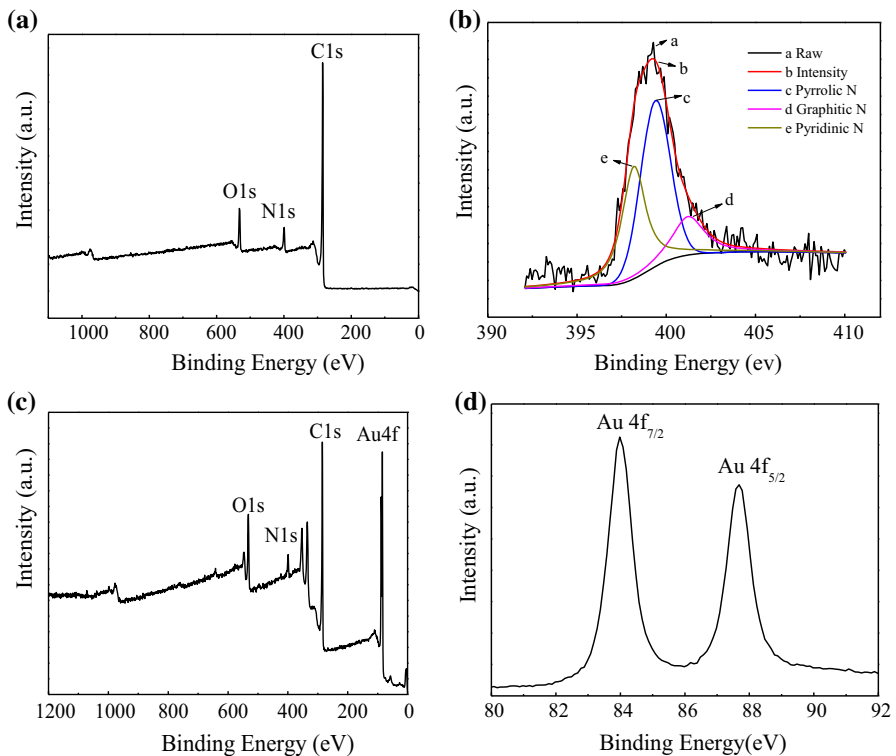


Fig. 4 XPS spectra of N-G (a) and Au/N-G NPs (c), high-resolution N 1s spectra of N-G (b), Au 4f of Au/N-G NPs (d)

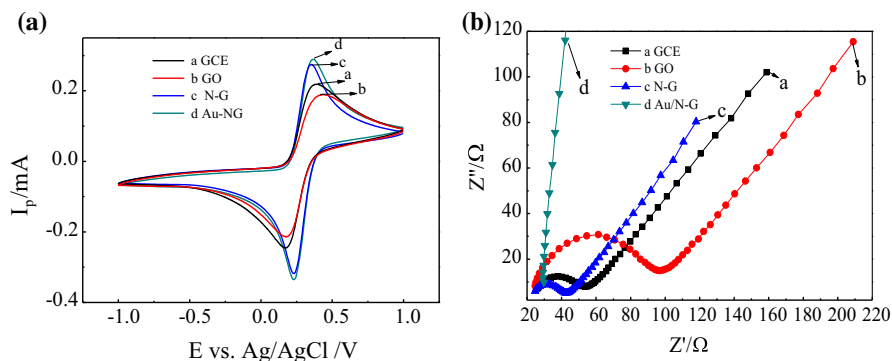


Fig. 5 The CV curves of different modified GCE at a scan rate of 100 mV s^{-1} (a) and the Nyquist plots of different modified GCE (b); bare GCE (a), GO/GCE (b), N-G/GCE (c), Au/N-G/GCE (d)

Electrochemical performance of N-G and Au/N-G NPs

The CV and EIS tests of different modified GCE were carried out in $\text{K}_2[\text{Fe}(\text{CN})_6]$ solution. As shown in Fig. 5a, all CV curves were symmetrical redox peaks. The bare GCE showed obvious redox peaks because of its certain electron transfer capacity (*curve a*). While the bare electrode was modified with GO or N-G, the redox peak current of GO/GCE decreased (*curve b*) in comparison with the bare GCE, but the peak current of N-G/GCE increased (*curve c*). After modification with Au/N-G (Au/N-G/GCE), the redox peak current of Au/N-G/GCE was higher than other modified electrodes (*curve d*).

The semicircle diameter at a higher frequency in the Nyquist diagram reflected the interfacial electron transfer resistance. As shown in Fig. 5a, the bare GCE displayed a small semicircle with a R_{et} value of about 46Ω at high frequency (*curve a*). In the next step, when the electrode was modified with GO, an increasing R_{et} value was observed, which was consistent with the result that oxygen-containing functional groups could hamper the electron transfer. After modification with N-G, the electrode exhibited a much lower resistance for the redox probe (*curve b*), because doping nitrogen can change its electronic properties and accelerate the electron transfer rates (*curve c*). In the final step, when the electrode was modified with Au/N-G NPs, electrons were easily transferred and the EIS curve exhibited a straight line (*curve d*). The electron transfer rates can be further improved owing to the synergistic effect between N-G and AuNPs, which suggested that Au/N-G NPs were a good conductive material.

Conclusions

In this work, we introduced $(\text{NH}_4)_2\text{CO}_3$ as a nitrogen resource to synthesize N-G via a hydrothermal process, and Au/N-G NPs were synthesized by a microwave irradiation method. The XPS analysis of N-G indicated that the nitrogen existed in

the form of pyridinic nitrogen, pyrrolic nitrogen and graphitic nitrogen. Au/N-G NPs exhibited good electrochemical properties due to the synergistic effect between AuNPs and N-G. Those results suggested that Au/N-G nanocomposite could be a promising material in the fields of catalysts and electrochemical sensors.

Acknowledgments This work was financially supported by the National Natural Science Foundation of China (No. 21106101), the National High Technology Research and Development Program of China (No. 201406017), and the Tianjin Youth Science Foundation (No. 13JCQNJC06300).

References

1. F. Schedin, A. Geim, S. Morozov, E. Hill, P. Blake, M. Katsnelson, K. Novoselov, *Nat. Mater.* **6**, 652 (2007)
2. K.S. Novoselov, D. Jiang, F. Schedin, T.J. Booth, V.V. Khotkevich, S.V. Morozov, A.K. Geim, *Proc. Natl. Acad. Sci.* **102**, 10451 (2005)
3. S.M. Li, S.Y. Yang, Y.S. Wang, C.H. Lien, H.W. Tien, S.T. Hsiao, *Carbon* **59**, 418 (2013)
4. T.O. Wehling, K.S. Novoselov, S.V. Morozov, E.E. Vdovin, M.I. Katsnelson, A.K. Geim, A.I. Lichtenstein, *Nano Lett.* **8**, 173 (2008)
5. M. Xing, W. Fang, X. Yang, B. Tian, J. Zhang, *Chem. Commun.* **50**, 6637 (2014)
6. K. Akada, T.O. Terasawa, G. Imamura, S. Obata, K. Saiki, *Appl. Phys. Lett.* **104**, 1 (2014)
7. Y. Fujimoto, S. Saito, *J. Appl. Phys.* **115**, 153701 (2014)
8. L.H. Wang, Z.Z. Zhang, B.J. Ding, Y. Guo, *Phys. Lett. A* **378**, 904 (2014)
9. L. Zhang, J. Niu, M. Li, Z. Xia, *J. Phys. Chem. C* **118**, 3545 (2014)
10. G. Dongsheng, Y. Songlan, Z. Yong, Y. Jinli, L. Jian, L. Ruying, S. Tsun-Kong, S. Xueliang, Y. Siyu, *S. Knights, Appl. Surf. Sci.* **257**, 9193 (2011)
11. D. Wei, L. Peng, M. Li, H. Mao, T. Niu, C. Han, W. Chen, A.T.S. Wee, *ACS Nano* **9**, 164 (2015)
12. Y.C. Lin, C.Y. Lin, P.W. Chiu, *Appl. Phys. Lett.* **96**, 133110 (2010)
13. D. Long, W. Li, L. Ling, J. Miyawaki, I. Mochida, S.H. Yoon, *Langmuir* **26**, 16096 (2010)
14. T. Cui, R. Lv, Z.H. Huang, H. Zhu, F. Kang, K. Wang, D. Wu, *Carbon* **50**, 3659 (2012)
15. Y. Xue, B. Wu, L. Jiang, Y. Guo, L. Huang, J. Chen, J. Tan, *J. Am. Chem. Soc.* **134**, 11060 (2012)
16. Z. Lin, G. Waller, Y. Liu, M. Liu, C.P. Wong, *Adv. Energy Mater.* **2**, 884 (2012)
17. L. Sun, L. Wang, C. Tian, T. Tan, Y. Xie, K. Shi, M. Li, H. Fu, *RSC Adv.* **2**, 4498 (2012)
18. Z. Hang, T. Kuila, K. Nam Hoon, V. Dong Sheng, L. Joong Hee, *Carbon* **69**, 66 (2014)
19. X. Xie, J. Long, J. Xu, L. Chen, Y. Wang, Z. Zhang, X. Wang, *RSC Adv.* **2**, 12438 (2012)
20. G. Yang, Y. Li, R.K. Rana, J.J. Zhu, *J. Mater. Chem. A* **1**, 1754 (2013)
21. P. Kannan, T. Maiyalagan, N.G. Sahoo, M. Opallo, *J. Mater. Chem. B* **1**, 4655 (2013)
22. X. Xu, Y. Zhou, T. Yuan, Y. Li, *Electrochim. Acta* **112**, 587 (2013)
23. V.M. Dhavale, S.S. Gaikwad, S. Kurungot, *J. Mater. Chem. A* **2**, 1383 (2014)
24. W.S. Hummers Jr, R.E. Offeman, *J. Am. Chem. Soc.* **80**, 1339 (1958)
25. N.I. Kovtyukhova, P.J. Ollivier, B.R. Martin, T.E. Mallouk, S.A. Chizhik, E.V. Buzaneva, A.D. Gorchinskiy, *Chem. Mater.* **11**, 771 (1999)
26. B. Xiong, Y. Zhou, Y. Zhao, J. Wang, X. Chen, R. O'Hayre, Z. Shao, *Carbon* **52**, 181 (2013)
27. G. Chang, H. Shu, Q. Huang, M. Oyama, K. Ji, X. Liu, Y. He, *Electrochim. Acta* **157**, 149 (2015)
28. H. Wang, M. Xie, L. Thia, A. Fisher, X. Wang, *J. Phys. Chem. Lett.* **5**, 119 (2014)